Effect of processing conditions on transient liquid phase sintering of premixed aluminium alloy powders

N. B. Dhokey[1*], V. A. Athavale[1], N. Narkhede[2], M. Kamble[2]

[1]*Department of Metallurgical Engineering, Govt. College of Engineering Pune 411005, India*
[2]*Aluminium Sintered Products Pvt. Ltd., Chakan, Pune, India*

[*]Corresponding author. Tel: (+91) 20-25507262, Fax: (+91) 20-25507299; E-mail: nbdhokey@yahoo.co.in

ABSTRACT

Aluminium powder metallurgy is attracting attention of many researchers for making near net shape components by replacing conventional process of liquid metallurgy. In the present work, sintering response of a 2xxx series aluminium powder premix, containing 4.5Cu-1Si-0.8Mg (by wt %) blended without any lubricant in a mixer with a ball to powder ratio of 10:1 (by wt) has been studied. The higher mixing time of 6 hours and compacting pressure of 450 MPa gave 90% theoretical sintered density and hardness of 91 HRH with uniform distribution of alloying elements and optimal dimensional growth. Copyright © 2013 VBRI press.

Keywords: Powder metallurgy; aluminium alloys; mixing time; compacting pressure.

Narendra B. Dhokey received Ph.D. from V.N.I.T Nagpur in 2007 and M.Tech.(Process Metallurgy) in 1995 from I.I.T. Mumbai. Presently he is working as Professor in Department of Metallurgical Engineering, Govt. College of Engineering Pune (India). He has published more than 40 papers in National and International Journal and conferences. He has 20 years of teaching experience including 6 years industrial experience in Steel plant. His main area of research is Synthesis of alloys, Powder Metallurgy, Cryogenic treatment of materials and Tribology of materials.

V. A. Athavale pursuing M. Tech. in Process Metallurgy from Department of Metallurgy and Materials Science, Government College of Engineering, Pune (India). He obtained B.E. in Production Engineering from Shivaji University, Kolhapur (India) in 2010. Presently, he is working as Research Assistant on Industry sponsored project at Government College of Engineering, Pune. His main research areas are Powder Metallurgy, Alloy Development and Powder Injection Moulding.

Introduction

Interest in aluminium P/M parts for the automobile industry has been drastically increased during last few years due to its cost effective nature which include typical automotive applications like connecting rods, camshaft bearing caps and sprocket for a camphaser system [1]. However, the major setback is due to the lack of availability of commercial alloys for such particular applications. Alternatively, alloys can be designed systematically using the phase diagram characteristics of ideal liquid phase sintering systems [2]. It was observed that sintering with participation of the liquid phase in aluminium-copper powder metallurgy parts undergo growth in the first stage of sintering and shrinkage in the second [3]. If the copper content in the mixture does not exceed the solubility limit in aluminium at sintering temperature, then powder metallurgy specimens undergo only growth since all of the copper is absorbed from the molten material by the solid phase and the liquid phase disappears. The extent of shrinkage depends upon the starting porosity [4]. It is noted that it is possible to improve sintering of pressed aluminium powders through the use of trace elements addition. These alloys show a marked improvement in strength and density to that of traditional press and sinter aluminium alloys. Specifically, the sintering response and subsequent material properties obtained using a typical 2xxx series alloy (Al-4.4Cu-0.8Si-0.5Mg) has been improved through the addition of Sn and modifying the sintering parameters viz. compacting pressures [5, 6]. During sintering, the liquid

phase flows between powder and particles and aid the densification by capillary action, particle rearrangement and enhanced mass transport where the particle size of powders plays a vital role in it [7]. Thermodynamically stable oxide layer limits the diffusion and hinders wetting and liquid spreading during sintering. Magnesium is known to react with oxide and it therefore plays a major role by disrupting oxide layer forming a spinel during the sintering of aluminium [8]. The dimensional growth varies with the type of atmosphere chosen; hence pure dry nitrogen atmosphere is suggested since it gives better sintered properties as compared to other atmospheres [1, 9-12]. The formation of AlN is the key effect which was believed to reduce the pressure in the closed pore, which unbalances the meniscus forces, induce pore filling [9]. It was observed that the mixing technique employed for blending of powders plays a vital role in homogeneous distribution of alloying elements and also for getting better sintered properties [13]. In this proposed research work, systematic effort has been made to improve the understanding on variation of mixing time and compacting pressure on the sinterability and the resulting mechanical properties of the sintered compacts of 2xxx series premixed alloy powders.

Experimental

Materials

Powder morphology of the elemental powders used in this work is observed in SEM as shown in **Fig. 1**. Aluminium powder exhibits irregular and ellipsoidal shape. Copper powder has dendritic structure while Silicon powder has rocky appearance and that Magnesium powder is flaky. The powder properties viz. apparent density, purity and particle size with their sources are listed in **Table 1**.

Synthesis of Sintered Compacts

All elemental powders of composition Al-4.5Cu-1Si-0.8Mg (by wt%) were blended in a ball mill having ball to powder ratio as 10:1 (by wt) for the duration of 1 hour to 6 hours so as to optimize the mechanical mixing time. No external lubricant was used while making premix. The particle size analysis was carried out by Laser particle analyser at IIT, Bombay to evaluate the average particle size and the effect of mixing time on the particle size of premix powders. And it was observed that the average particle size of 6 hours blended powder was 94 μm as revealed from **Fig. 2**. Blended premix powders were compacted at 150 MPa and 450 MPa to evaluate and compare their effect on sintered properties of resultant premixes. For every mixing time, samples with dimensions 12 mm diameter x 8 mm height were prepared. The sintering temperature and time was fixed at 560 ^{0}C and 30 min respectively since it promotes transient liquid phase formation in the initial stage of sintering. After predetermined sintering period, specimens were cooled by water quenching method. The complete sintering cycle followed is depicted in **Fig. 3**.

Compression test

Compression testing was carried on three specimens of each mixing time and for each compacting pressure in UTM (10T). The specimen was gradually pressed in compression in steps of 50 Kg, and its instantaneous height and diameter were recorded to get true stress verses true strain plot as per flow curve equation (1), using the average of three test specimens.

$$\sigma = K . \varepsilon^{n} \qquad (1)$$

where, σ = True stress in MPa; K= Strength coefficient, MPa; ε= True strain, mm/mm; n= strain hardening exponent.
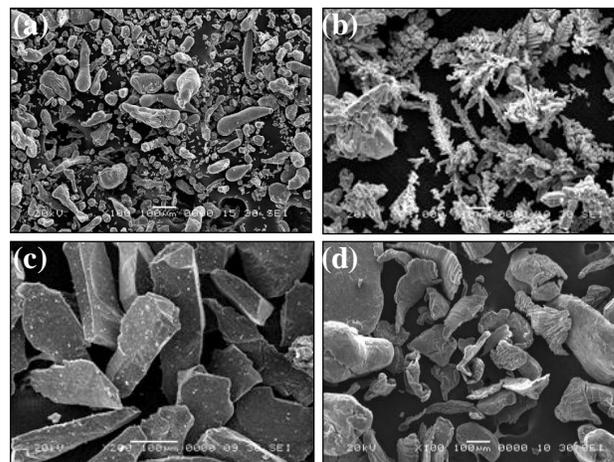
Fig. 1. SEM morphology of (a) Aluminium (b) Copper (c) Silicon and (d) Magnesium powders.

Table 1. Powder properties and their sources.

Sr. No	Type of powders	Apparent density, g/cc	Purity, %	Particle size Mesh (μm)	Source of Powders
1	Aluminum Powder	1.16	99.60	170 (90 μm)	Komal Atomizer, Mumbai
2	Copper powder (E)	1.62	99.60	325 (45 μm)	Industrial Metal Powders (India) Pvt Ltd, Pune
3	Silicon Powder	0.96	98.50	170 (90 μm)	Research Lab Fine Chem. Industries, Mumbai
4	Magnesium Powder	0.64	99.50	270 (53 μm)	Research Lab Fine Chem. Industries, Mumbai
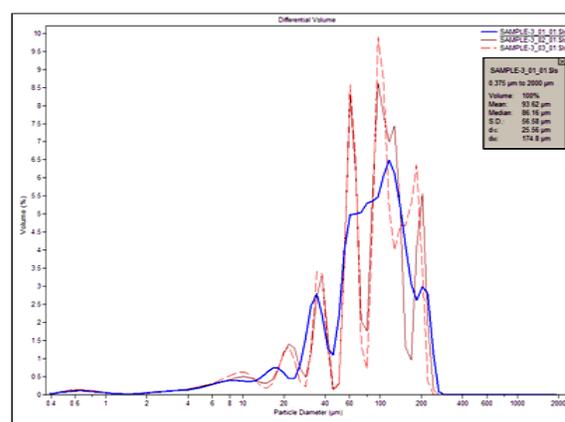
Fig. 2. Laser particle analysis of premix alloy powder 4.5Cu-1Si-0.8Mg (by wt %) (Mixing time 6 hours).
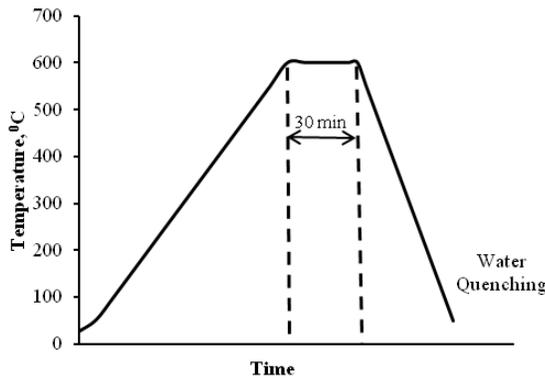
Fig. 3. Complete sintering cycle followed for sintering of premix alloy powder.

Metallography

Microstructures were observed using inverted optical microscope (make-Carl Zeiss). Scanning Electron Microscope (SEM) and Energy Dispersive Spectroscopy (EDS) techniques (make-JEOL, Japan) were employed for observing phases and alloying elemental distribution. Samples for SEM analysis were polished by using electrolytic polishing machine (make- Eletropol Metatech) with a flow of electrolyte solution (Methanol-730 mL, Butyl Cellosolve-98mL, Perchloric acid-78mL and Distilled water- 100 mL). Additionally, for revealing grain boundaries of matrix, the etching was carried out using Keller's reagent (Nitric Acid- 2.5 mL, Hydrochloric Acid- 1.5 mL, Hydrofluoric Acid- 1.0 mL, Distilled Water- 95 mL). XRD analysis was done by XPERT-PRO X-ray diffractometer (Copper target, K-alpha-1.5406 ^{0}A) to confirm the phases formed during sintering. Bulk hardness was taken using Rockwell H-scale (HRH) with a 60 kg load and 1/8 inch ball indenter. The dimensions (height and diameter) were measured using digital micrometer (make-Mitutoyo) having least count of 1 μm. Diameter was checked at three positions top, middle and end along longitudinal direction. Hardness and dimensional changes reported in this report resulted from average of 3 readings per sample for three specimens.

Results and discussion

Density variation

Fig. 4 shows the effect of mechanical mixing time and compacting pressures on the green density of the premixes. There is no remarkable increasing trend for lower compacting pressure. But on the other hand, higher compacting pressure results in decrease in green density with increase in mixing time. The reason behind this could be attributed to lower mixing time thereby giving less strained particles while higher mixing time gives more strained particles. These strained particles may oppose compaction pressure hence decrease in green density at 450 MPa.

But the opposite trend was observed in case of sintered density as evident in **Fig. 5**. The higher compacting pressure gives higher sintered density due to more driving force for sintering which has resulted from residual stresses introduced during mechanical mixing. **Fig. 6** depicts total porosity, that is, 16 % at 150 MPa and 10 % at 450 MPa

respectively. Overall, there is no appreciable effect of mixing time on variation in porosity. It may be noted that the maximum green density is obtained for the specimen compacted at 450 MPa and 1 hour mixing time but maximum sintered density (90% Theoretical density) is obtained for the specimen compacted at 450 MPa and 6 hours mixing time.
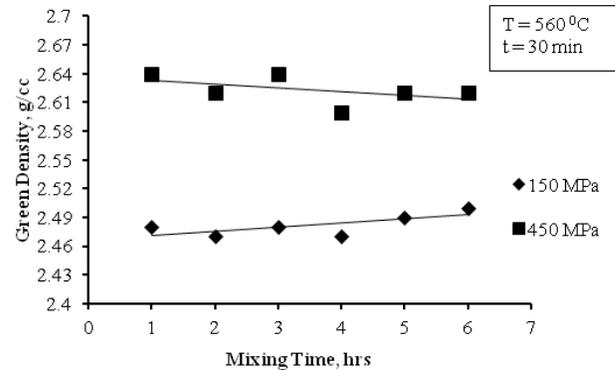
Fig. 4. Effect of mechanical mixing time and compacting pressures on the green density of premixes.
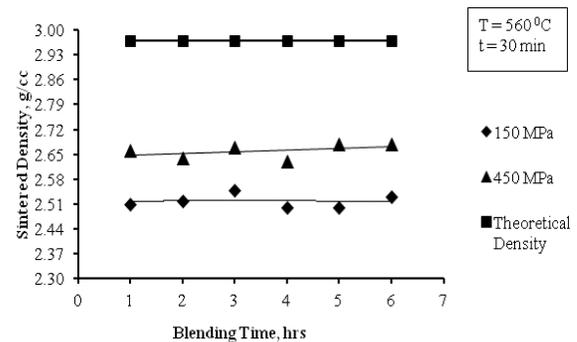
Fig. 5. Effect of mixing time and compacting pressures on the sintered density of the premix.
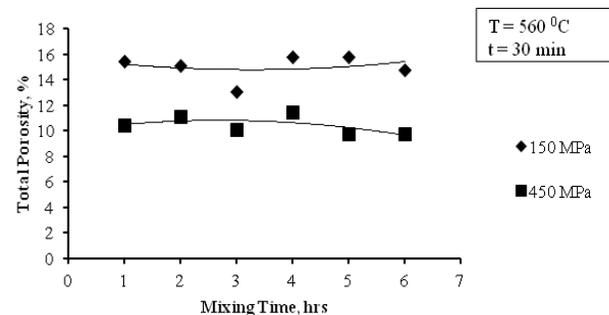
Fig. 6. Effect of mixing time on variation of total porosity.

Dimensional growth

The variation in longitudinal and radial growth is shown in **Fig. 7** and **8**, respectively. At higher compacting pressure of 450 MPa, the longitudinal growth increases up to 3 hours mixing time and then falls and similar nature is seen for radial growth.   The longitudinal growth remains unaffected at 150 MPa, but radial growth gradually increases with increasing mixing time and then falls. It is evident that the longitudinal and radial growth is below 1%, which was assumed to be an acceptable limit for aluminium alloys for all the mixing time employed. These dimensional

changes cannot be compared with the densification parameter. It was reported that [**4**]; the growth of samples is significant if it contains impurities.
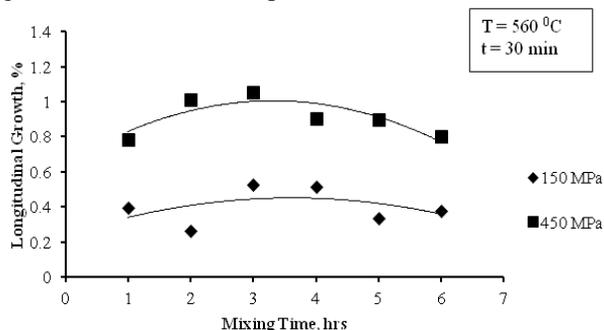
Fig. 7. Variation in longitudinal growth for samples compacted at 150 and 450 MPa.
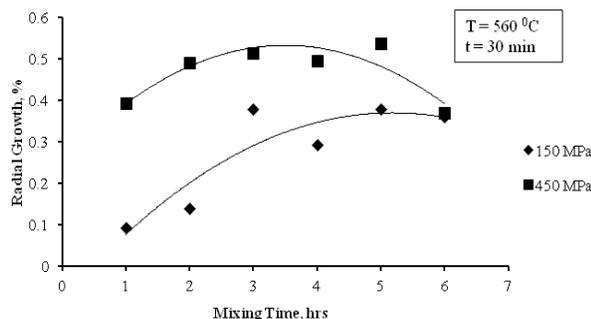
Fig. 8. Variation of radial growth in samples as a function of mixing time.

Hardness variation

Increasing mixing time gives higher hardness due to improved sinterability as a result of inherent residual stresses which acts as driving force for sintering. The maximum hardness of 91 HRH is seen at 6 hours mixing time. The gradual increase of hardness is observed as evident from **Fig. 9.** With increase in mixing time, it enhances the diffusion of atoms across the particle interface due to transient eutectic liquid phase [**15**] (M.P. 548 ^{0}C) formed at sintering temperature of 560 ^{0}C.
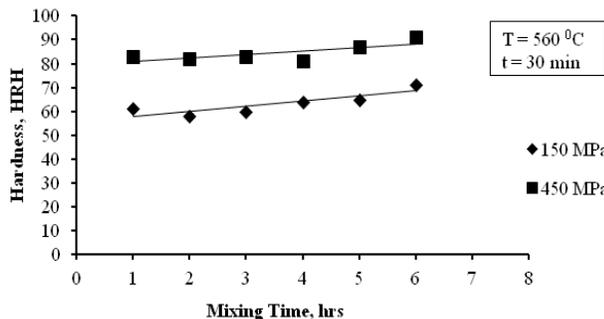
Fig. 9. Hardness variation with mixing time for varying compacting pressure.

Microstructural features

The porosity was relatively more for samples having mixing time 1 hour than 6 hours which is clearly visible from SEM microstructure of both the specimen as shown in **Fig. 10**. Also EDS pattern of both the samples shows that elements are homogeneously distributed when mixed for 6 hours as depicted in **Fig. 12** and some segregation of

elements like copper as indicated in **Fig. 11**. There is a major difference between the mutual diffusivities of Al and Cu [**15**]. Faster diffusivity of copper in aluminium enhances the rate of homogenisation; it causes expansion via Kirkendall effect [**2,6,14**]. It is evident that the enhanced diffusion of copper is seen for 6 hours mixing time of powder that can be attributed to large driving force which normally comes from cold welding of the particles during mechanical milling. This gives appreciable homogenisation of alloying elements especially Copper and Silicon as depicted in **Fig. 12**. However, the mixing time of 1 hour is not adequate enough to homogenize copper as evident in **Fig. 11**. Also, it is observed from **Fig. 10** that the particle boundaries are fully merged with lesser porosity whereas porosity is prominently observed for lower mixing time compact.
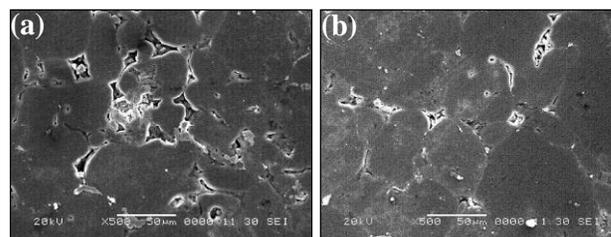
Fig. 10. SEM images comparing sinterability of samples compacted at 450 MPa and sintered at 560^{0}C for a) 1 hour mixing, b) 6 hours mixing time.
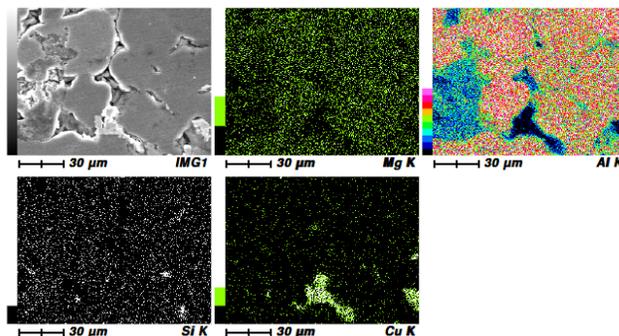
Fig. 11. Elemental distribution of 1 hour mixed sample compacted at 450 MPa and sintered at 560^{0}C showing segregation of elements.
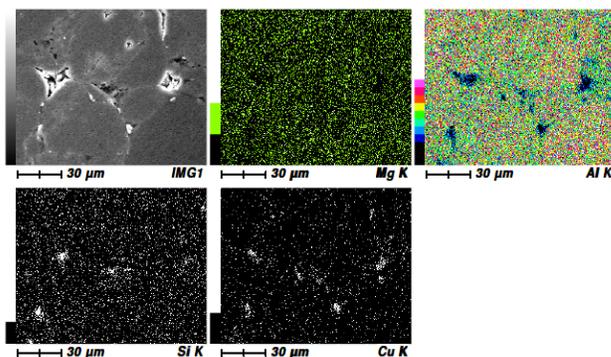
Fig. 12. Elemental distribution of 6 hours mixed sample compacted at 450 MPa and sintered at 560 ^{0}C.

The liquid phase formation is necessary for effective sintering of aluminium alloys. Above 548 ^{0}C, the liquid

phase formed is eutectic. If sufficient time is permitted then the liquid gets completely absorbed in aluminium matrix [**14**] and promotes growth. With increasing mixing time, the alloying elements start distributing homogeneously. Simultaneously, the particles get finer for higher mixing time. It was reported that formation of coarser particles gives more liquid phase whereas finer particles gives lesser liquid phase [**7**].
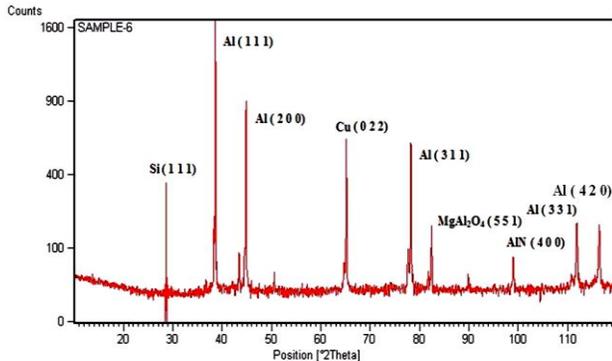
Fig. 13. XRD graph for sintered compact (mixing time 3 hrs, compacting pressure 450 MPa, sintered at 560 ^{0}C for 30 min and water quenched).
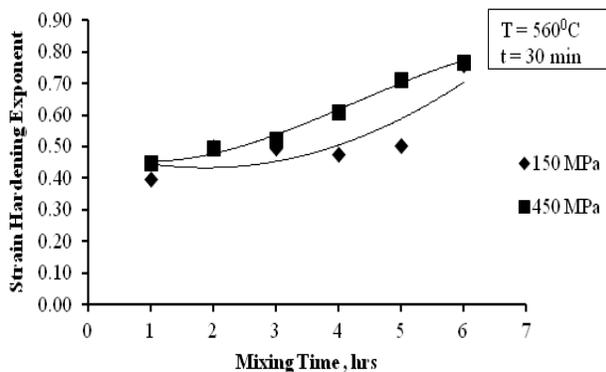
Fig. 14. Effect of mixing time on strain hardening exponent of the sintered compact.

XRD analysis

XRD analysis was carried out to find out the effect of alloying elements and sintering parameters on the sinterability of aluminium powder and precipitation of any allied phases as noted in **Fig.13**. And it was observed that Magnesium reacts with aluminium oxide and formed the spinel ($MgAl_2O_4$). Besides, the formation of AlN is noted due to its negative free energy of formation [**16**]. Similar observation has been observed by other researcher [**8**].

Flow curve properties

The flow curve properties plotted in **Fig. 14** provides useful information on strain hardening rate of the sintered compact. It is evident that strain hardening exponent increases with increasing mixing time. It indicates strengthening to the sintered component is caused by the diffusion of the atomic species which goes with increasing mixing time. The compacting pressure does play very crucial role in improving the sinterability of the sintered component. This does not show significant change in

crushing load characteristics at higher compacting load of 450 MPa for the level of mixing time as depicted in **Fig. 15**. However, low compacting load of 150 MPa makes some level of improvement in crushing load. It can be concluded that it is necessary to optimize the process variables to control the sintered properties of the specimen.
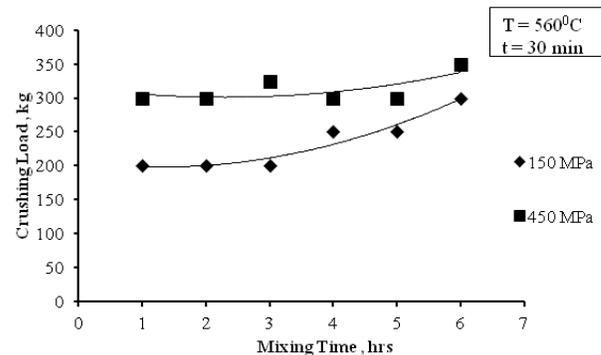
Fig. 15. Effect of mixing time on crushing load of the sintered compact.

Conclusion

The proposed premix of powders containing 4.5wt%Cu; 1wt%Si; 0.8wt%Mg and balance Aluminium were compacted at selected pressures and effect of mixing time on powders were established. The following are the conclusions drawn from the analysis-

a)   The mixing time shows direct linear correlation with sintered density. The maximum response to sintered density (90% Theoretical Density) is obtained at 450 MPa.

b)   Both radial and longitudinal growths are affected by mixing time of the powders. However, growth is less than 1 % for the given sintering time and temperature due to homogeneous distribution of alloying elements.

c)   The hardness and mixing time shows linear correlation. The maximum hardness of 91 HRH is obtained for compacting pressure of 450 MPa.

d)   The strain hardening exponent is slightly affected by the mixing time whereas crushing load remains steady at 450 MPa for almost entire duration of mixing time.

e)   The alloying element particularly copper is uniformly distributed for the 6 hours mixing time whereas some segregation of copper is observed due to inadequate mixing time of 1 hour during mechanical alloying.

Reference

1.   Pieczonka, T.; Schubert, Th.; Baunack, S.; Kieback, B. Mater. Sci. Eng. A. 2008, *478*, 251.
    DOI: 10.1016/j.msea.2007.06.002

2.   Schaffer, G.; Sercombe, T.; Lumley, R. Mater. Chem. and Phy. **2001**, *67*, 85.
    PII: S0254-0584(00)00424-7

3.   Savitskii, A.; Romanov, G.; Gopienko, V. Poroshkovaya Metallurgiya, **1988**, *307*, 70. Translated by Plenum Publication Corporation.

4. Savitskii, A.; Romanov, G. Poroshkovaya Metallurgiya, **1987**, *295*, 22. Translated by Plenum Publication Corporation.
5. Schaffer, G.; Sercombe, T. Acta Mater. **1999**, *47*, 689.
   PII: S1359-6454(98)00353-X
6. Lefebvre, L.; Thomas, Y.; White, B. J. Light Metals, **2002**, *2*, 239.
   DOI: 10.1016/S1471-5317(03)00007-5
7. Lumley, R.; Schaffer, G. Scripta Mater. **1996**, *35*, 589.
   PII: S1359-6462(96)00195-9
8. Sercombe, T.; Lumley, R.; Schaffer, G. Metall. Mater. Trans. A. **1999**, *30 A*, 457.
9. Schaffer, G.; Hall, B.; Bonner, S.; Huo, S.; Sercombe, T. Acta Mater. **2006**, *54*, 131.
   DOI: 10.1016/j.actamat.2005.08.032
10. Schaffer, G.; Yao, J.; Bonner, S.; Crossin, E.; Pas, S.; Hill, A. Acta Mater. **2008**, *54*, 2615.
    DOI: 10.1016/j.actamat.2008.01.047
11. MacAskill, I.; Hexemer, R.; Donaldson, I.; Bishop, D. J. Mater. Process. Tech. **2010**, *210*, 2252.
    DOI: 10.1016/j.jmatprotec.2010.08.018
12. Martin, J.; Castro, F. J. Mater. Process. Tech. **2003**, *143-144*, 814.
    DOI: 10.1016/S0924-0136(03)00335-2
13. Dhokey, N.; Athavale, V.; Narkhede, N.; Kamble, M. Adv. Mat. Lett. Article in Press, **2013,** *4(2)*, 164.
    DOI: 10.5185/amlett.2012.6369
14. Delgado, M.; Ruiz-Navas, E.; Gordo, E.; Torralba, J. J. Mater. Process. Tech. **2005**, *162-163*, 280.
    DOI: 10.1016/j.jmatprotec.2005.02.037
15. ASM Handbook, *Alloy Phase Diagrams*, ASM International, Materials Park, OH, **1992**, Vol. 3, pp. 291-292, 305-306, 322.
16. Kubaschewski, O. *Metallurgical Thermochemistry*, Fifth ed., Maxwell Macmillan International Edition, **1989**, pp. 378.